nature cell biology

PIASy mediates NEMO sumoylation and NF-κB activation in response to genotoxic stress

Angela M. Mabb[1], Shelly M. Wuerzberger-Davis[1] and Shigeki Miyamoto[1,2]

Protein modification by SUMO (small ubiquitin-like modifier) is an important regulatory mechanism for multiple cellular processes[1,2]. SUMO-1 modification of NEMO (NF-κB essential modulator), the IκB kinase (IKK) regulatory subunit, is critical for activation of NF-κB by genotoxic agents[3]. However, the SUMO ligase, and the mechanisms involved in NEMO sumoylation, remain unknown. Here, we demonstrate that although small interfering RNAs (siRNAs) against *PIASy* (protein inhibitor of activated STATy) inhibit NEMO sumoylation and NF-κB activation in response to genotoxic agents, overexpression of PIASy enhances these events. PIASy preferentially stimulates site-selective modification of NEMO by SUMO-1, but not SUMO-2 and SUMO–3, *in vitro*. PIASy–NEMO interaction is increased by genotoxic stress and occurs in the nucleus in a manner mutually exclusive with IKK interaction. In addition, hydrogen peroxide (H_2O_2) also increases PIASy–NEMO interaction and NEMO sumoylation, whereas antioxidants prevent these events induced by DNA-damaging agents. Our findings demonstrate that PIASy is the first SUMO ligase for NEMO whose substrate specificity seems to be controlled by IKK interaction, subcellular targeting and oxidative stress conditions.

We previously showed that SUMO-1 modification of NEMO–IKKγ is required for the activation of NF-κB in response to etoposide (VP16) and camptothecin (CPT), but not by lipopolysaccharide or tumor necrosis factor α (TNFα)[3]. This sumoylation is associated with nuclear accumulation of IKK-free NEMO and is followed by phosphorylation on Ser 85 by ATM (ataxia telangiectasia mutated), which is required for activation of IKK and NF-κB in the cytoplasm[4]. To identify a SUMO ligase critical for NEMO, an siRNA screen was performed against known SUMO ligases. HEK293 cells transfected with siRNAs were treated with VP16 and lysates were analysed for NF-κB activation by electrophoretic mobility shift assay (EMSA). To evaluate the specificity of siRNAs, total RNA was also isolated and RT–PCR was performed for *SUMO E3* mRNAs. This analysis demonstrated minimal off-target effects for the *SUMO E3* siRNAs used (Fig. 1a).

Only *PIASy* siRNAs exhibited inhibition of NF-κB by VP16, but not TNFα (Fig. 1b, and see Supplementary Information, Fig. S1a). SiRNAs against Ran-binding protein 2 (*RanBP2*), another SUMO E3 (ref. 5), did not inhibit NF-κB activation by VP16 (data not shown). The use of two individual *PIASy* siRNA oligonucleotides showed a dose dependent decrease in PIASy protein levels that correlated with reductions in NF-κB activation (Fig. 1c). *PIASy* siRNAs also inhibited NF-κB activation by other DNA damaging agents, including CPT, ionizing radiation, doxorubicin and ultraviolet irradiation (Fig. 1d), and in HeLa human cervical cancer cells and CEM human T leukemic cells (data not shown). *PIASy* siRNAs also caused inhibition of NF-κB-dependent luciferase reporter gene activity to the same extent as those against *Ubc9*, the gene encoding the only known SUMO E2 (Fig. 1e). Combination of *PIASy* and *Ubc9* siRNAs did not further reduce reporter activity (Fig. 1e). Finally, *PIASy* siRNAs also prevented NF-κB-dependent induction of endogenous target genes, such as *IL-8* and *IκBα* in HEK293 cells (Fig. 1f and see Supplementary Information, Fig. S1b, c) and *p21* (ref. 6) in CEM cells (see Supplementary Information, Fig. S1d).

As anticipated, *PIASy* siRNAs prevented NEMO sumoylation induced by VP16 (Fig. 2a). They did not interfere with the activation of ATM, as measured by the decrease in the reactivity to phospho-Ser 1981-ATM, a specific antibody[7] (Fig. 2b). Consistent with Ser 85 phosphorylation being downstream of NEMO sumoylation[4], *PIASy* siRNAs blocked this phosphorylation event (Fig. 2c). Overexpression of PIASy resulted in both increased basal and VP16-inducible NEMO sumoylation (Fig. 2d) and NF-κB activation (Fig. 2e). In contrast, overexpression of a catalytically inactive mutant PIASy, ($PIASy^{CA}$ with the catalytic Cys 342 and Cys 347 mutated to alanine)[8] inhibited VP16-inducible sumoylation of NEMO and NF-κB activation (Fig. 2f, g).

To examine whether PIASy can function as a direct SUMO E3 for NEMO, amino-terminally HA-tagged NEMO substrate was *in vitro* translated in rabbit reticulocyte extracts in the presence of ^{35}S-methionine and then incubated with sumoylation reaction mixtures containing recombinant sumoylation components. Of the four major bands translated (see Supplementary Information, Fig. S2a), only the slowest migrating band could be immunoprecipitated with an anti-HA antibody. Thus, this band represents the full-length HA–NEMO protein,

[1]Program in Molecular and Cellular Pharmacology, Department of Pharmacology, University of Wisconsin, Madison, WI 53706, USA.
[2]Correspondence should be addressed to S.M. (e-mail: smiyamot@wisc.edu)

Received 21 April 2006; accepted 6 June 2006; published online 13 August 2006; DOI: 10.1038/ncb1458

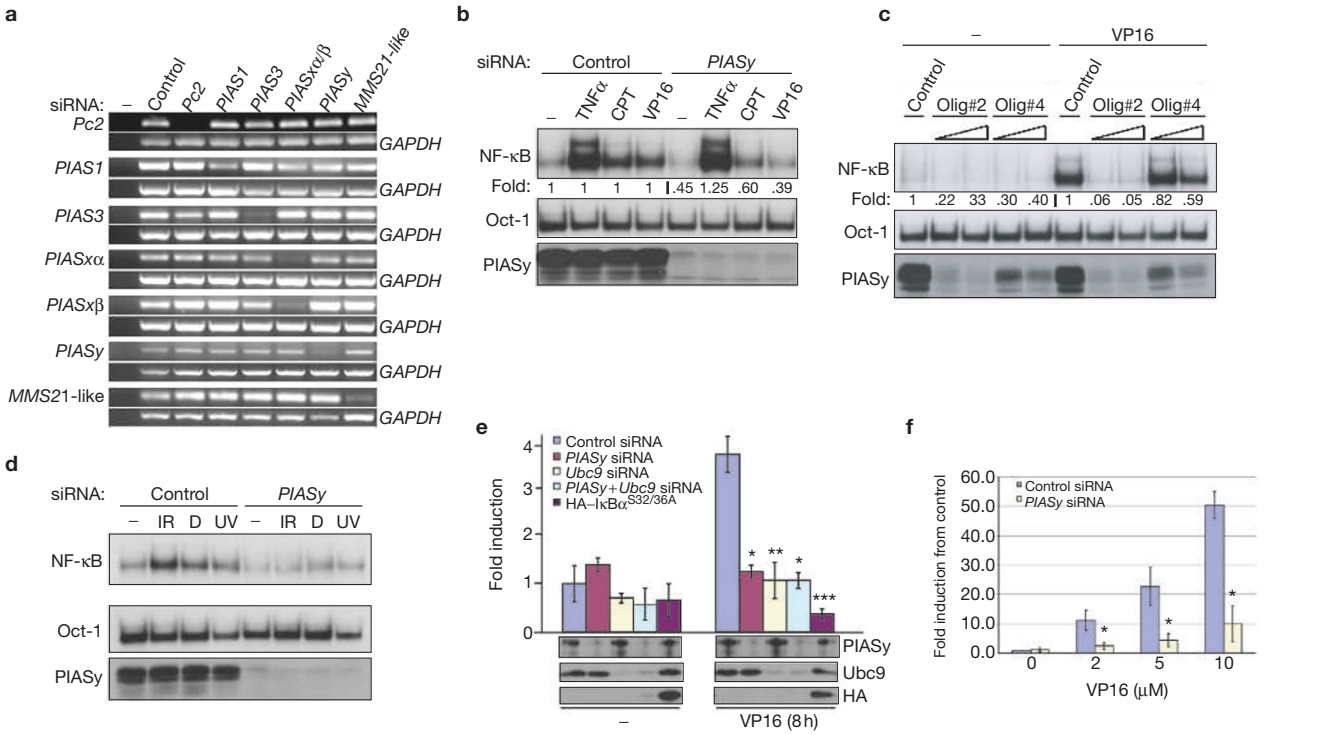

Figure 1 PIASy is necessary for NF-κB activation by genotoxic agents. (**a**) HEK293 cells were transfected with control or siRNAs against genes encoding different SUMO ligases. RNA was isolated and the expression level of mRNA for each SUMO ligase was determined using RT–PCR. GAPDH served as a loading control. (**b**) HEK293 cells were transfected as stated above with control or *PIASy* siRNAs. Cells were treated with 10 ng ml^{-1} TNFα for 15 min, 10 μM VP16 for 90 min and 10 μM CPT for 120 min. Total cell extracts were made and NF-κB activity was measured by EMSA. EMSA with an Oct-1 probe was used as a control. Western blots of total protein extracts were probed with anti-PIASy antibody. (**c**) HEK293 cells were transfected with control or two different siRNA oligonucleotides against *PIASy* (oligo #2 and oligo #4). Cells were treated with 10 μM VP16 for 90 min. Total cell extracts were analysed as in **b**. (**d**) HEK293 cells were transfected as stated in **a**. Cells were treated with 20 Gy of ionizing radiation (IR) for 90 minutes, 25 μM doxorubicin (D) for 105 minutes and 60 J m^{-2} UV (254 nm) for 135 minutes. Total cell extracts were analysed as in **b**. (**e**) HEK293 cells were transfected twice with control siRNA, *PIASy* siRNAs, *Ubc9* siRNAs, or the super-repressor IκBα$^{S32/36A}$ along with 3× *κB–Luc NF-κB* reporter gene and 24 h after the second transfection cells were treated with VP16 for 8 h. The cell extracts were used for the luciferase assay and relative luciferase activities were plotted by comparing fold induction with untreated control. Western blots of the same cell extracts with anti-PIASy, anti-Ubc9,and anti-HA antibodies are also shown to demonstrate knockdown efficiency. Means±s.d. are shown (n=3). Mean values were compared to the VP16-treated control siRNA using an unpaired t-test and determined to be statistically significant. *, P <0.04; **, P <0.03; ***, P <0.01. (**f**) HEK293 cells were transfected with control or *PIASy* siRNAs and treated as stated above with increasing doses of VP16. RNA was analysed for *IL-8* expression using quantitative real time RT–PCR. Means±s.d. are shown (n=4). Median values were compared to the VP16-treated control siRNA using the Mann-Whitney Rank Sum test and determined to be statistically significant. *, P <0.03. An uncropped scan of the top gel in **b** is shown in the Supplementary Information, Fig. S5a.

whereas the smaller bands may represent translation products derived from internal methionines or degradation products. After the sumoylation reaction, three major slower-migrating bands were observed (see Supplementary Information, Fig. S2b), of which the two highest bands could be immunoprecipitated with an anti-HA antibody. These bands also reacted with anti-NEMO and anti-SUMO-1 antibodies when analysed by western blotting (data not shown), indicating that they are sumoylated full-length NEMO species. The nature of the third band could not be determined by these analyses.

When Flag–PIASy expressed in and immunopurified from HEK293 cells was added to the *in vitro* sumoylation reaction under the conditions in which the sumoylation of NEMO was minimal with only E1 and E2 (Fig. 3a), an enhancement of NEMO sumoylation was observed that was dependent on all components of the reaction mixture. Similarly prepared PIASy^{CA} failed to enhance NEMO sumoylation. Quantification of enhancement in repeated experiments demonstrated a 2.5-fold enhancement by PIASy, but not by PIASy^{CA}.

In accordance with the immunopurified PIASy described above, recombinant human His–PIASy purified from *Escherichia coli* showed enhancement of NEMO sumoylation *in vitro* (not shown). However, we were unable to purify it to near homogeneity. Thus, a recombinant *Xenopus* PIASy protein that shares 77% sequence identity and 84% homology with the human protein (His–xPIASy, Fig. 3d) and that was previously described for *in vitro* sumoylation of topoisomerase II, was used[9]. His–xPIASy, purified to near homogeneity, enhanced sumoylation of *in vitro* translated NEMO, which showed major bands similar to those observed with FLAG–PIASy (Fig. 3c), as well as high molecular weight smears or ladders. All modified NEMO species could be cleaved by the catalytic domain of recombinant SENP1, a SUMO protease (Fig. 3c). Importantly, His–xPIASy promoted SUMO-1 isoform-specific modification of NEMO, similar to genotoxic stress conditions *in vivo*[3], as it failed to efficiently sumoylate NEMO in the presence of SUMO-2 or SUMO-3 (see Supplementary Information, Fig. s2e). A similar result was obtained using His–NEMO protein expressed in *E. coli* and purified to near homogeneity (Fig. 3d, e). Thus, these results demonstrated that PIASy enhanced SUMO-1 modification of NEMO in a highly purified *in vitro* system. In addition, overexpression of *Xenopus* PIASy could enhance NF-κB activation in HEK293 cells and could also

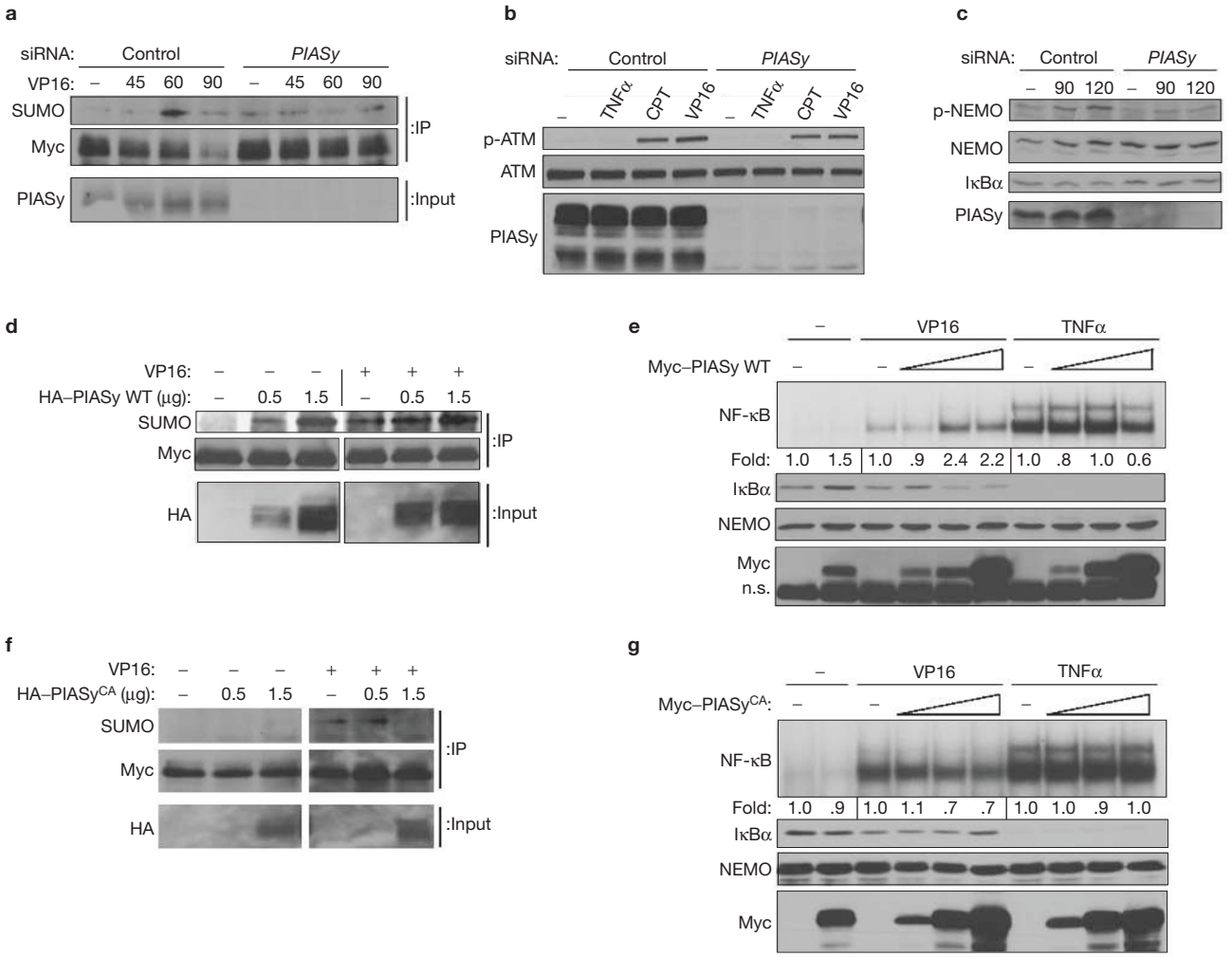

Figure 2 PIASy modulates NEMO sumoylation and NF-κB activation in response to genotoxic stress. (**a**) HEK293 Myc–NEMO stable cells were transfected with control or *PIASy* siRNAs. Cells were left untreated or treated with 10 μM VP16 for indicated times in minutes. Cell lysates were boiled in 1% SDS and 10% input samples were taken. The remaining samples were then diluted to 0.1% SDS and immunoprecipitated with anti-Myc antibody. The precipitates were blotted with anti-SUMO-1 and anti-Myc antibodies. Inputs were blotted with anti-PIASy antibody. (**b**) HEK293 cells were transfected with control or *PIASy* siRNAs and treated with 10 ng ml^{-1} TNFα for 15 min, 10 μM CPT for 75 min or 10 μM VP16 for 60 min. Total cell extracts were examined by immunoblotting with an anti-ATM and anti-phospho-Ser 1981-ATM antibodies. PIASy protein was examined by immunoblotting with an anti-PIASy antibody. (**c**) HEK293 cells were transfected as stated in **b** and treated with 10 μM VP16 for the indicated times. Total cell extracts were examined by immunoblotting with an anti-phospho-Ser 85-NEMO, anti-NEMO, anti-IκBα and anti-PIASy antibodies. (**d**) HEK293 Myc–NEMO stable cells were transfected with 0.5 and 1.5 μg of a PIASy expression vector. Cells were left untreated or treated with 10 μM VP16 for 60 min. Cell lysates were prepared and immunoprecipitated as in **a**. The precipitates were blotted with anti-SUMO-1 and anti-Myc antibodies. 10% inputs were blotted with anti-HA antibody. (**e**) HEK293 cells were transfected with 0.5, 1.5 and 4.0 μg of a PIASy expression vector. Cells were treated with 10 μM VP16 for 60 min and 10 ng ml^{-1} TNFα for 15 min. Total cell extracts were measured for NF-κB activity by EMSA. Cell lysates were probed with anti-IκBα, anti-NEMO and anti-Myc antibodies. n.s., nonspecific band. (**f**) HEK293 Myc–NEMO stable cells were transfected with a $PIASy^{CA}$ expression vector. Cells were processed as in **a**. Precipitates were blotted as in **d**. (**g**) HEK293 cells were transfected with 0.5, 1.5 and 4.0 μg of a $PIASy^{CA}$ expression vector. Cells were analysed as in **e**. An uncropped scan of the top gel in **a** is shown in the Supplementary Information, Fig. S5b.

partially rescue the *PIASy* siRNA-induced inhibition of NF-κB activation in response to VP16 (see Supplementary Information, Fig. 2c, d), indicating that *Xenopus* PIASy can functionally compensate for endogenous human PIASy in a mammalian cellular environment.

NEMO sumoylation in response to genotoxic agents is blocked by mutations of Lys 277 and Lys 309 (ref. 3). To determine whether PIASy could promote sumoylation on these residues, sumoylation assays were performed using $NEMO^{K277A}$ and $NEMO^{K309A}$ mutants in the presence of His–xPIASy (Fig. 3f, g). Whereas K277A mutagenesis prevented the formation of one of the sumoylated bands (open circle) and caused an apparent increase in sumoylation of another band (closed circle), $NEMO^{K309A}$ lost the slower migrating of the two sumoylated bands (closed circle). These results suggested that the upper of the two bands represented sumoylated NEMO on Lys 309 and the lower band on Lys 277. When both lysines were mutated ($NEMO^{DK}$), the two bands migrated differently from those seen in the wild-type NEMO protein (single and double stars). Thus, it is likely that mutation of Lys 277 and Lys 309 results in sumoylation of NEMO on alternative sites. Although these lysine residues conform to the optimal sumoylation site, ψKxE (where ψ represents a hydrophobic amino acid and x represents any amino acid)[10,11], both of these sites partially deviate from this sequence due to the presence of alanine at position 276 and aspartate at

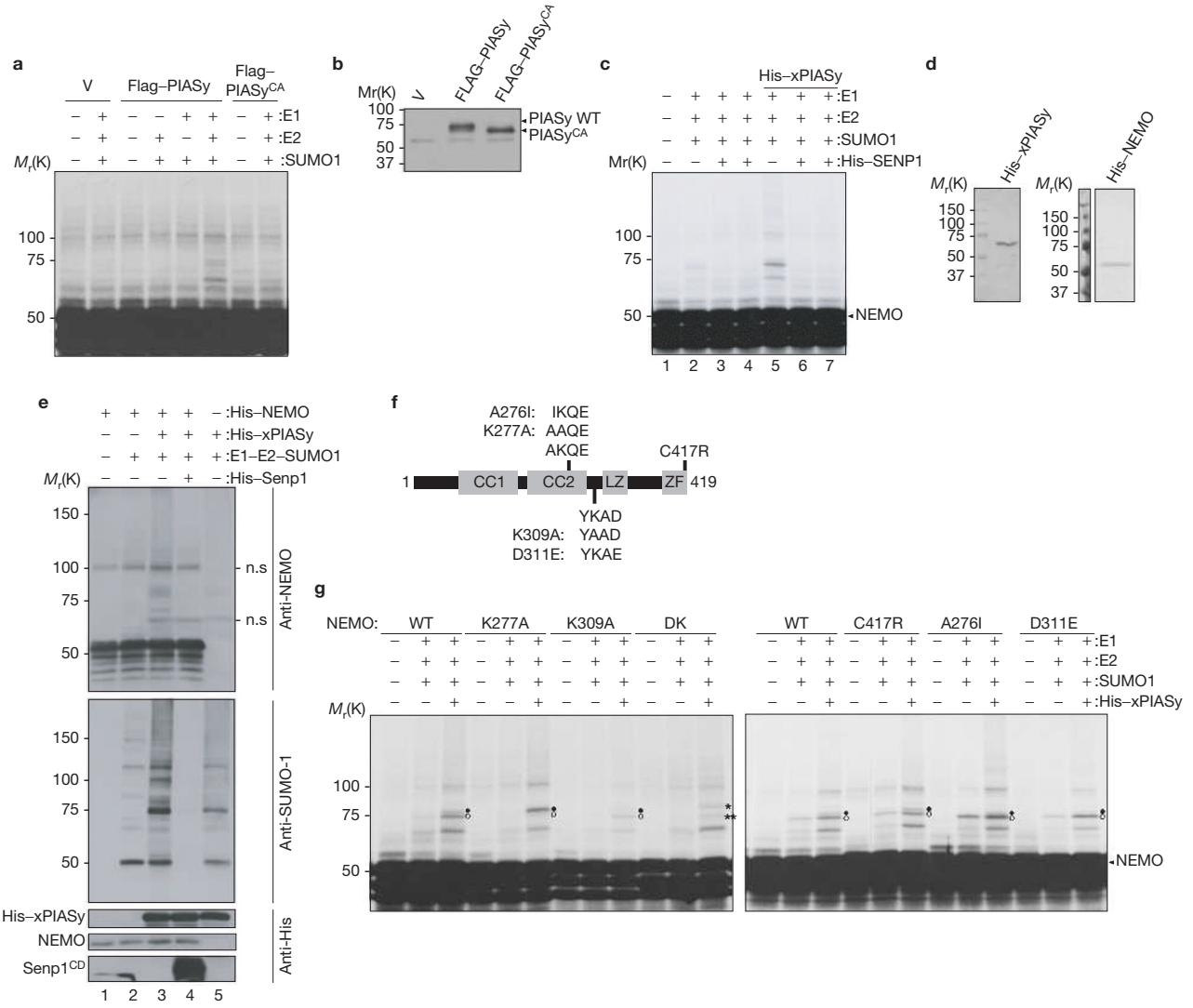

Figure 3 PIASy promotes sumoylation of NEMO *in vitro*. (**a**) HEK293 cells were transfected with Flag–PIASy WT and CA constructs or vector control (V). Cell lysates were immunoprecipitated with an anti-Flag antibody and washed extensively using high salt buffer. Immunopurified PIASy WT and CA beads were then added to the *in vitro* sumoylation assay containing *in vitro* translated ^{35}S HA–NEMO, and the reaction mixtures were incubated at 30 °C for 90 min. Reaction products were separated by SDS–PAGE and the dried gel was exposed to an X-ray film. (**b**) Anti-Flag western blot showing immunopurified Flag–PIASy WT and CA mutant, and vector control used for the *in vitro* assay in **a**. (**c**) *In vitro* sumoylation assay was performed with *in vitro* translated ^{35}S HA–NEMO and 0.5 μg of recombinant His–xPIASy for 75 min at 30 °C. Recombinant His–SENP1 (0.75 and 1.5 μg in lanes 6 and 7, respectively) was added after *in vitro* sumoylation to cleave the SUMO-1 moiety from modified NEMO. Reactions were terminated in 2× SDS sample buffer, run on an SDS–PAGE gel, fixed and exposed to film. (**d**) Commassie stained gels of recombinant *Xenopus* His–xPIASy and recombinant human His–NEMO. (**e**) *In vitro* sumoylation assay was performed using 0.75 μg of recombinant His–NEMO and 1 μg of recombinant His–xPIASy at 30 °C for 75 min. His–SENP1 was added after sumoylation in lane 4. Samples were terminated in 2× SDS sample buffer, run on an SDS–PAGE gel and blotted with anti-NEMO, anti-SUMO-1 and anti-His antibodies. (**f**) Schematic representation of the NEMO mutants used in **g**. CC1, coiled-coil 1; CC2, coiled-coil 2; LZ, leucine zipper; ZF, zinc finger. The positions of mutated amino-acid residues are indicated. (**g**) *In vitro* sumoylation assay was performed as in **a** with the addition of *in vitro* translated ^{35}S-methionine labelled HA–NEMO mutants K277A, K309A, K277A/K309A (DK), C417R, A276I and D311E and using recombinant His–xPIASy as in **c**. Closed circle indicates SUMO-1 modification of NEMO putatively at Lys 309, open circle indicates SUMO-1 modification of NEMO putatively at Lys 277 and * and ** represent SUMO-1 modification of NEMO at unidentified sites.

position 311 (Fig. 3f). To further examine site-selective sumoylation *in vitro*, Ala 276 was mutated to isoleucine to create a more hydrophobic residue at the –1 position. This resulted in increased sumoylation of the putative Lys 277 band compared with wild-type NEMO (Fig. 3g). In contrast, when Asp 311 was mutated to glutamate, sumoylation of the Lys 309 band was not greatly affected, suggesting that PIASy promotes sumoylation of NEMO at Lys 309 equivalently with either aspartate or glutamate at the +2 position. Mutations within the carboxy-terminal zinc finger domain of NEMO severely hinder NEMO sumoylation and NF-κB activation by genotoxic stress inducers[3]; however, a NEMO zinc-finger mutant (NEMO^{C417R}) was efficiently sumoylated by PIASy (Fig. 3g). Hence, the intact zinc finger is not necessary for direct NEMO sumoylation by PIASy. Similar results were obtained for all of the NEMO mutants with immunopurified human Flag–PIASy (see Supplementary Information, Fig. 3a).

To test whether PIASy interacts with NEMO *in vivo*, HA–PIASy was transfected into HEK293 cells and endogenous NEMO was immunoprecipitated following exposure to VP16. A modest amount of HA–PIASy

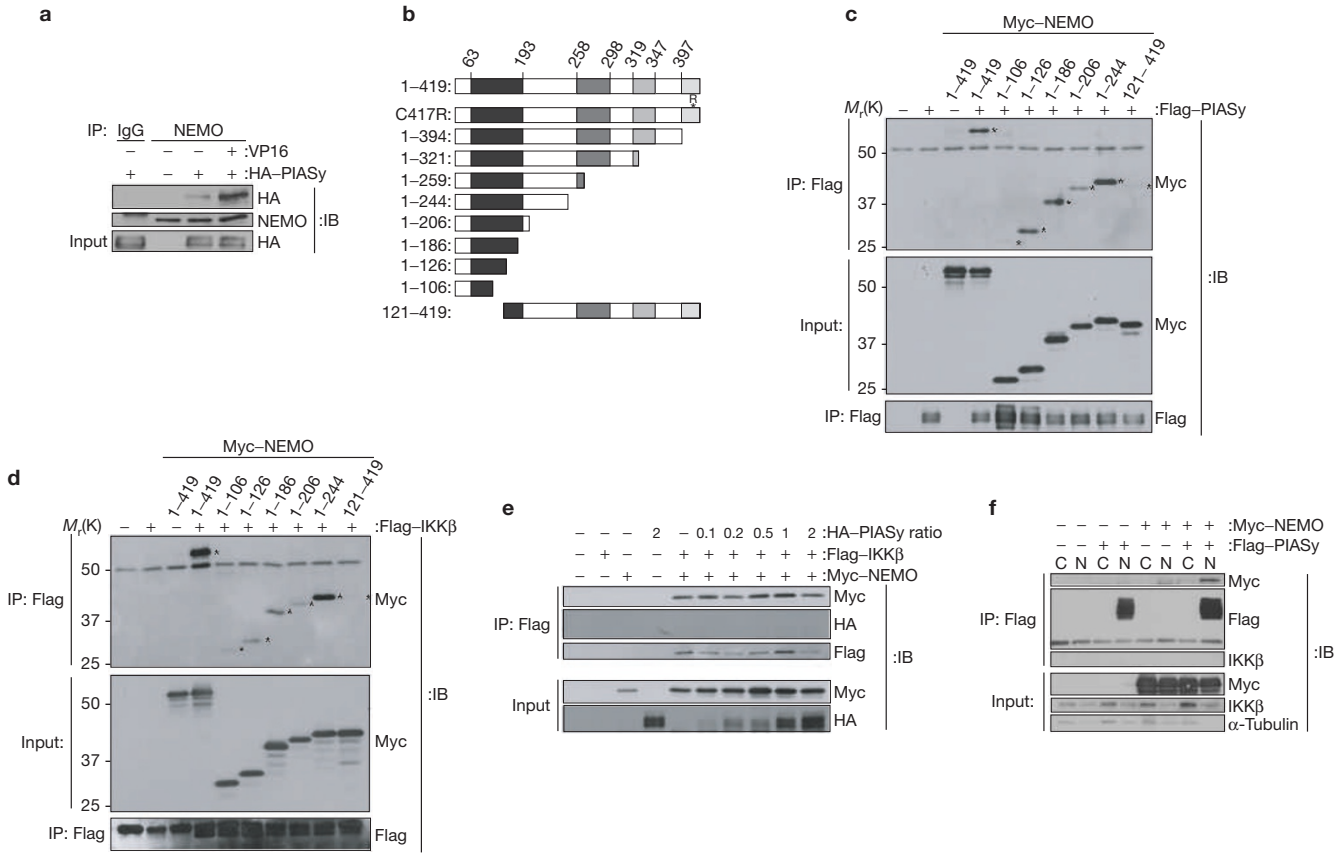

Figure 4 NEMO interacts with PIASy in a manner that is mutally exclusive with IKKβ binding. **(a)** HEK293 cells were transfected with HA–PIASy or empty vector. Lysates were immunoprecipitated with anti-NEMO antibody or a mouse IgG control. Samples were immunoblotted with anti-HA and anti-NEMO antibodies. (**b**) Schematic representation of NEMO mutants used for coimmunoprecipitation analysis with human Flag–PIASy and human Flag–IKKβ. Amino acids 63–193 represent coiled-coil 1 (CC1), 258–298 represent coiled-coil 2 (CC2), 319–347 represent a leucine zipper and 397–418 represent a zinc finger. (**c**) HEK293 cells were transfected with Flag–PIASy and Myc–NEMO mutants. Cells extracts were immunoprecipitated with an anti-Flag antibody and probed with an HRP-conjugated anti-Myc antibody. 2% input was also probed with anti-Myc antibody. (**d**) HEK293 cells were transfected with Flag-IKKβ and Myc–NEMO mutants. Extracts were immunoprecipitated as in **c**. (**e**) HEK293 cells were transfected with Flag-IKKβ, Myc–NEMO and increasing amounts of HA–PIASy construct. Cell extracts were immunoprecipitated with an anti-Flag antibody and probed with anti-Flag and HRP-conjugated anti-HA and anti-Myc antibodies. Immunoblots with 2% inputs are also shown. (**f**) HEK293 cells were transfected with Flag–PIASy, Myc–NEMO or empty vector. Cytoplasmic and nuclear extracts were isolated and PIASy was immunoprecipitated with anti-Flag antibody. Samples were immunoblotted with anti-Flag, anti-Myc, anti-IKKβ and anti-tubulin antibodies.

was present in NEMO precipitates without any stimulation (Fig. 4a and see Supplementary Informtaion, Fig. S3b) and this interaction was further augmented on treatment with VP16. Myc–NEMO mutants (Fig. 4b) and Flag–PIASy were co-expressed and their interactions were examined to determine the region(s) of NEMO that are critical for PIASy interaction. Successive C-terminal deletions demonstrated that NEMO$^{1-126}$ was sufficient to interact with PIASy (Fig. 4c and see Supplementary Information, Fig. S3c). A deletion of the first 120 amino-acid residues of NEMO abrogated its interaction with PIASy. These results showed that the amino terminus of NEMO is both necessary and sufficient for PIASy association.

The N-terminal region of NEMO is also essential for IKKβ interaction[12]. Coimmunoprecipitation experiments with NEMO mutants and Flag–IKKβ demonstrated that association of the NEMO mutants with IKKβ was nearly identical to interaction with PIASy (Fig. 4d). Cotransfection and coimmunoprecipitation experiments further demonstrated that NEMO–PIASy and NEMO–IKK interactions are mutually exclusive (Fig. 4e and see Supplementary Information, Fig. S3d). Moreover, subcellular fractionation studies revealed a NEMO–PIASy complex in the nuclear fraction, but the majority of IKKβ was located in the cytoplasm (Fig. 4f). Even though a small amount of IKKβ was observed in the nuclear fraction under these conditions, an IKKβ–PIASy interaction was not detected. These results suggested that PIASy–NEMO interaction occurs predominantly in the nucleus in a manner mutually exclusive with NEMO–IKKβ interaction.

As many double-strand break (DSB)-inducing agents also induce oxidative stress[13–16], we examined whether such a stress could be critical for NEMO sumoylation and NF-κB activation. The antioxidants N-acetylcysteine (NAC) and pyrrolidinedithiocarbamate (PDTC) prevented sumoylation of endogenous NEMO and NF-κB activation without interfering with ATM activation in response to VP16 (Fig 5a, b) and CPT (data not shown) in CEM cells. Moreover, the pro-oxidant H_20_2 was capable of promoting NEMO sumoylation, which was sensitive to inhibition by antioxidants (Fig. 5c). H_20_2 also promoted PIASy–NEMO interaction (Fig. 5d). Taken together, these findings suggested the possibility that oxidative stress may be critical for induction of a PIASy–NEMO interaction and NEMO sumoylation after exposure to certain DNA-damaging agents.

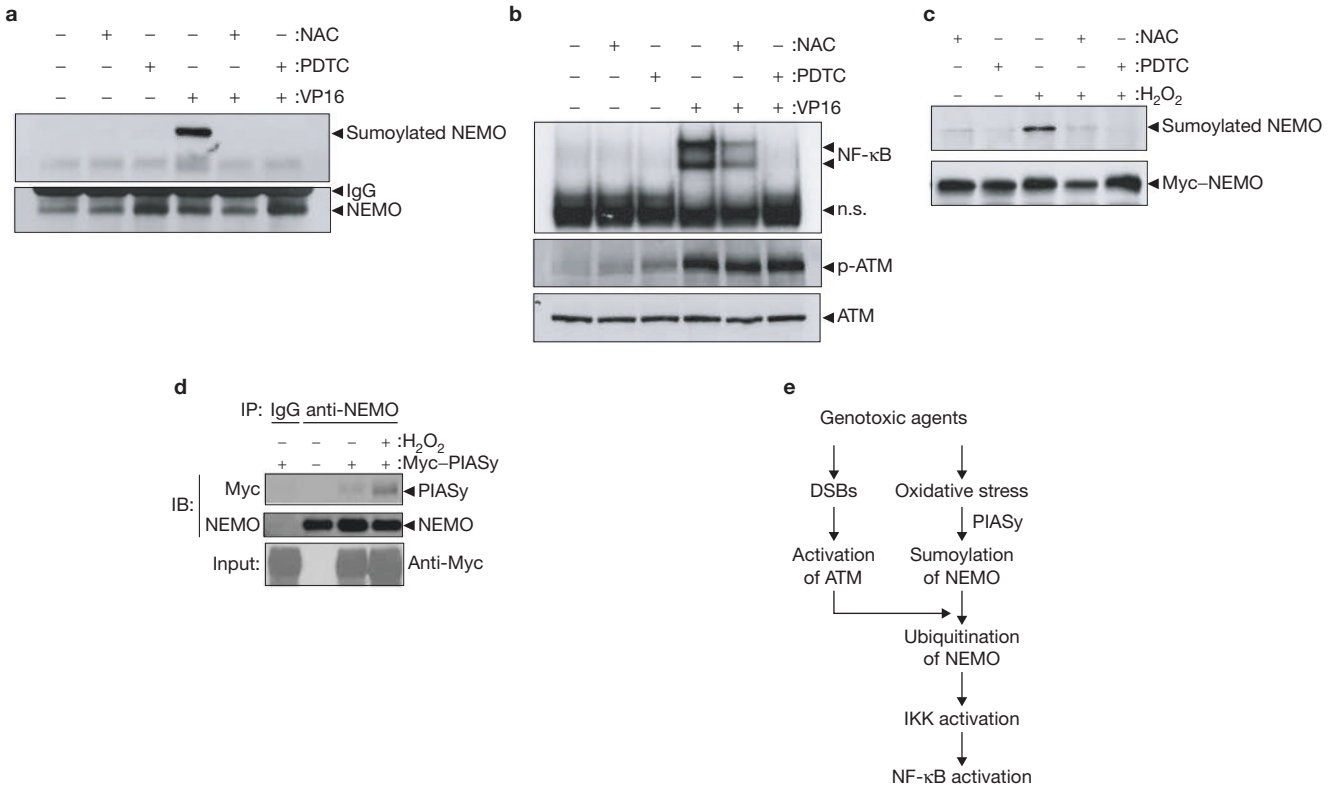

Figure 5 Oxidative stress seems to be required for NEMO sumoylation in response to VP16. (**a**) CEM cells were pretreated for 3 h with 50 mM NAC and for 30 min with 100 μM PDTC. Cells were then treated for 1 h with 10 μM VP16. Cell lysates were boiled in 1% SDS and then diluted to 0.1% SDS and immunoprecipitated with anti-NEMO antibody. Precipitates were immunoblotted with anti-SUMO-1 and anti-NEMO antibodies. (**b**) CEM cells were treated as above and cell lysates were analysed by EMSA and western blotted with an anti-ATM and anti-phospho-Ser 1981-ATM antibodies. (**c**) 1.3E2 NEMO-deficient murine pre-B cells stably expressing Myc–NEMO were pretreated with NAC and PDTC as above. Cells were treated with 2mM H_2O_2 for 45 min. Cell lysates were immunoprecipitated with anti-Myc antibody and precipitates were immunoblotted with anti-SUMO-1 and anti-Myc antibodies. (**d**) HEK293 cells were transfected with Myc–PIASy and 24 h later they were treated with 2 mM H_2O_2 for 45 min. Cell lysates were immunoprecipitated with an anti-NEMO antibody and the precipitates were immunoblotted with HRP-conjugated anti-Myc and anti-NEMO antibodies. (**e**) Schematic representation of a model for genotoxic stress-induced NF-κB activation. Genotoxic agents cause both DSBs and oxidative stress. DSBs lead to ATM activation, whereas oxidative stress may promote NEMO–PIASy interaction and NEMO sumoylation. These parallel events together promote NEMO ubiquitination and activation of IKK and NF-κB. An uncropped scan of the top gel in **a** is shown in the Supplementary Information, Fig. S5c.

In summary, we have shown that PIASy meets the minimal requirements of a SUMO ligase for NEMO in the genotoxic stress-induced NF-κB signalling pathway. First, a reduction of the expression of endogenous PIASy by siRNAs reduces the cellular capacity to cause SUMO-1 modification of NEMO and activate NF-κB in response to several DNA-damaging agents. Reduction of PIASy expression also attenuates NF-κB-dependent induction of both reporter and endogenous target genes without interfering with ATM activation. Second, overexpression of wild-type PIASy augments both basal and genotoxic stress-inducible sumoylation of NEMO and NF-κB activation. In contrast, a catalytically inactive PIASy mutant blocks NEMO sumoylation and NF-κB activation in response to genotoxic stimuli. Third, purified recombinant PIASy promotes modification of NEMO by SUMO-1, but not SUMO-2 or SUMO-3. *In vitro* sumoylation of NEMO by PIASy is also sensitive to mutations of Lys 277 and Lys 309, residues that are also necessary for *in vivo* sumoylation in response to genotoxic stress. Fourth, PIASy inducibly interacts with NEMO in response to DNA-damaging agents *in vivo*. Thus, these studies identify PIASy as the first SUMO E3 for NEMO relevant to the genotoxic stress NF-κB signalling pathway (Fig. 5e).

Our study also provides additional unexpected observations. A previous study using an RNAi screen against all putative ubiquitin proteases present in the human genome identified only CYLD (cylindromatosis tumor suppressor protein) as functioning in cytokine signalling[17]. Similarly, our RNAi screen against *SUMO E3s* found that only siRNAs against *PIASy* had inhibitory effects on NF-κB activation by genotoxic stress inducers. In contrast, some of the other E3s tested showed reproducible increases in NF-κB activation (for example, PIAS1 and PIAS3). It is unclear how these siRNAs cause this increase, but PIAS1 and PIAS3 have been shown to cause inhibition of p65 DNA binding activity[18,19]. Although we cannot exclude the possibility that other SUMO E3s also contribute to NEMO sumoylation in specific cellular contexts, our study demonstrates that PIASy is critical for NF-κB activation by genotoxic agents in multiple cell types.

In addition, we found that the N-terminal domain of NEMO is both necessary and sufficient for PIASy interaction. Interestingly, this overlaps with the region of NEMO where IKKβ associates[12]. IKKβ and PIASy fail to coimmunoprecipitate in the presence of NEMO, suggesting that NEMO–PIASy and NEMO–IKKβ complexes are mutually exclusive. The interaction between NEMO and PIASy is largely nuclear, as opposed to the IKKβ–NEMO interaction that is mostly cytoplasmic[12]. Thus, cell compartmentalization is an additional means to segregate these complexes. Our previous study indicated that IKK-free NEMO

becomes sumoylated and SUMO-modified NEMO accumulates in the nucleus[3]. The mutually exclusive interactions between NEMO–IKKβ and NEMO–PIASy partly explain why only IKK-free NEMO is targeted for sumoylation *in vivo*.

Nuclear interaction of PIASy–NEMO and increased basal sumoylation and NEMO nuclear accumulation (data not shown) on PIASy overexpression also suggest that NEMO sumoylation may occur in the nuclear compartment. As SUMO–NEMO fusion proteins displayed tendencies to accumulate in the nucleus, SUMO modification was suggested to promote NEMO nuclear targeting[3]. The zinc finger domain of NEMO was required for both sumoylation and nuclear targeting, further suggesting that this domain is required for sumoylation to take place. However, our current data demonstrate that the zinc finger is not required for NEMO interaction with PIASy *in vivo* or sumoylation *in vitro*. Instead, it may be critical for events involved in oxidative-stress signalling to promote NEMO nuclear localization[4] (Fig. 5e) or PIASy interaction of NEMO that is already located in the nucleus[20]. Alternatively, the zinc-finger domain may be necessary for stabilization of sumoylated NEMO, possibly by interfering with its interaction with a SUMO protease. PIDD (p53-inducible death domain) and RIP1 (receptor interacting protein 1) may be involved in the regulation of nuclear accumulation and sumoylation of NEMO in a manner dependent on the zinc-finger domain[20]. As activation of NF-κB by a variety of anti-cancer DNA-damaging agents is linked to modulation of malignant behaviours[21,22] (including resistance to chemo- and radiation therapy), further understanding of the enzymatic components and mechanisms involved may facilitate the development of novel anti-cancer agents targeting this signalling pathway. □

METHODS

Reagents. Etoposide (VP16), camptothecin (CPT), doxorubicin, 2, 5-diphenyloxazole (PPO), phenylmethylsulphonylfluoride (PMSF), aprotinin, N-acetylcysteine, N-ethylmaleimide and iodoacetamide were obtained from Sigma (St Louis, MO). Pyrrolidinedithiocarbamate was obtained from Alexis Corporation (Lausanne, Switzerland). Human recombinant TNFα and anti-tubulin antibody were obtained from Calbiochem (La Jolla, CA). Antibodies for horseradish peroxidase (HRP)-conjugated anti-goat, IκBα, c-Myc and NEMO were obtained from Santa Cruz (Santa Cruz, CA). Anti-c-Myc and anti-HA peroxidase antibodies were obtained from Roche (Indianapolis, IN). Anti-NEMO antibody was obtained from BD Pharminogen (San Jose, CA). Anti-Flag antibody was obtained from Sigma. Anti-GMP-1 (SUMO-1) and SUMO-2 antibodies was obtained from Zymed Laboratories (San Francisco, CA). ATM antibody was purchased from Genetex (San Antonio, TX) and anti-phospho-ATM (Ser 1981) was obtained from R & D Systems (Minneapolis, MN). Horseradish peroxidase (HRP)-conjugated anti-rabbit, anti-mouse antibodies, Gamma Bind G-Sepharose beads and protein G–Sepharose beads were obtained from Amersham (Piscataway, NJ). SUMO-1 antibody, human recombinant SUMO-1, SUMO-2, SUMO-3, *Saccharomyces cerevisiae* SUMO E1 (Aos1p/Uba2p), human recombinant SUMO E2 (Ubc9) and human recombinant His–SENP1 catalytic domain (CD) proteins were purchased from Boston Biochem (Cambridge, MA).

Cell culture. HEK293 and CEM cells were maintained as previously described[23]. HEK293 6× Myc–NEMO and 1.3E2 6× Myc–NEMO stable cell lines were generated as previously described[24].

siRNAs, RNA isolation and RT–PCR. siRNA-mediated knockdown of polycomb 2 (*Pc2*), *PIAS1*, *PIAS3*, *PIASxα/β*, *PIASy* and *MMS21*-like was performed by calcium phosphate transfection of 200 pmol of siGENOME SMARTpool double-stranded RNA oligonucleotides (Dharmacon, Lafayette, CO) or control siRNA (Dharmacon). A second transfection was also performed after 24 h to increase RNA interference efficiency. RNA from these transfected cells was isolated using the QIAshredder and RNeasy mini kits (Qiagen, Valencia, CA) 24 h after the second transfection. Multiplex RT–PCR was performed using Qiagen's OneStep RT-PCR kit according to the manufacturers' protocol. RT–PCR primers and siRNA oligonucleotide sequences are provided in the Supplementary Information, Fig. S4.

Cloning of PIASy and NEMO wild type and mutants. Generation of pcDNA3.1(+) 6×Myc–NEMO and pcDNA3.1(+) 2×HA–NEMO was described previously[24]. His–NEMO was cloned into pET-28a(+) from Novagen (Madison, WI) using restriction sites *Hind*III and *Xho*I. PcDNA3.1(+) 2×HA–NEMO A276I and D311E mutants were generated using site directed mutagenesis from pcDNA3.1(+) 2×HA–NEMO template. pcDNA3 2×HA–NEMO K277A and K309A mutants were generated through subcloning of pcDNA3 6×Myc–NEMO K277A and K309A (ref. 3) into pcDNA3 2×HA (Invitrogen) vector using restriction sites *BamH*I and *Xba*I. Flag-, Myc- and HA-tagged full-length PIASy was cloned through PCR amplification of PIASy from ATCC (Mammalian Genome Collection, Manassa, VA; IMAGE ID: 5176540) into pFlag–CMV-2 (Sigma) using *Not*I–*Xba*I restriction sites. PIASy was cloned into pcDNA3.1(+) 6×Myc (a gift from Z. Chen, UT-Southwestern, Dallas, TX) and pcDNA3.1(+) 2×HA constructs using *BamH*I–*Eco*RI restriction sites. PIASy C342/347A (CA) mutant was generated using two-step PCR mutagenesis from the original PIASy template. Primers used for cloning are available on request. All constructs were verified by DNA sequencing. *Xenopus* pET28a–PIASy was subcloned into the pcDNA3–Myc3 vector using *Eco*RI and *Xho*I restriction sites. Generation of a Flag–IKKβ construct was previously described[24].

Western blotting, immunoprecipitation and EMSA. Cell lysates production and western blotting was performed as previously described[25]. EMSA analysis and image quantification was also performed as previously described[26]. For NEMO–PIASy immunoprecipitations, cell lysates were precleared overnight with Gamma Bind G Sepharose. Precleared lysates were then immunoprecipitated as previously described[26].

Luciferase reporter assay. HEK293 cells were transfected with 25 ng of 3×κB–Luc, 25 ng of CMV–β-Gal, and 200 pmol of *PIASy* siRNA or control siRNA as stated above. Cells were treated with 10 μM VP16 for 8 h and harvested according to Promega's luciferase assay system kit. β-galactosidase activity was measured using the Galacton-Plus kit purchased from Tropix (Bedford, MA). The transfection efficiency was normalized within each cell line with β-galactosidase activity. Results were displayed as fold induction from untreated control.

Quantitative RT–PCR analysis. HEK293 cells were transiently transfected with control and *PIASy* siRNA as stated above and treated with increasing doses of VP16 for 3 h. Generation of total RNA from treated cells, cDNA synthesis from total RNA and quantitative real-time RT–PCR was previously described[6]. PCR primers used in this study are provided in the Supplementary Information, Fig. S4. Product accumulation was monitored by SYBR green fluorescence, with the relative expression levels determined from a standard curve of serial dilutions of cDNA. All samples were normalized to GAPDH levels and results were displayed as fold induction from untreated control.

Purification of recombinant His–NEMO. His–NEMO protein was generated in BL21 Rosetta 2 strain cultured in LB broth containing 25 μg ml^{-1} kanamycin and 34 μg ml^{-1} chloramphenicol. Cultures were induced at A_{600} = 0.5 with 1 mM IPTG for 3 h at 37 °C. Cell pellets were resuspended in equilibration/wash buffer (50 mM sodium phosphate, 300 mM NaCl at pH 7.0) and were lysed by sonication (4 rounds of 10 s bursts on ice). Cell debris and inclusion bodies were removed by centrifugation. The resulting supernatant was added to BD Talon Co^{2+} metal affinity resin (BD Biosciences). Bound protein was washed three times in equilibration/wash buffer and eluted in equilibration/wash buffer containing 150 mM imidazole. His–NEMO protein was then dialysed against 50 mM Tris at pH 7.6 and 5 mM $MgCl_2$.

***In vitro* and *in vivo* sumoylation assays.** *In vitro* sumoylation of NEMO was performed by *in vitro* translation of HA–NEMO protein using the TNT T7 Coupled Reticulocyte Extract System (Promega) in the presence of Redivue ^{35}S-methionine (Amersham). *In vitro* sumoylation assays were performed using 7.5 μg ml^{-1} SUMO E1 (Aos/Uba1), 50 μg ml^{-1} SUMO E2 (Ubc9) and 50 μg ml^{-1} of SUMO-1 added to 4 μl of *in vitro* translated NEMO in the presence of an ATP regenerating system (10 mM creatine phosphate, 10 units creatine kinase, 1 unit inorganic pyrophosphatase and 2 mM ATP) in 50 mM Tris at pH 7.6 and 5 mM $MgCl_2$

in a 40 μl reaction with 1 μg ml^{-1} aprotinin and 1 mM PMSF. The reaction was incubated at 30 °C for 180 min. End products were terminated with SDS sample buffer and separated by SDS–PAGE gels. Sumoylated products were detected by fixing SDS–PAGE gels in acetic acid followed by addition of the scintillant PPO. Gels were dried and exposed to autoradiograph film (Kodak, Rochester, NY). For *in vitro* sumoylation with recombinant His–NEMO and His–xPIASy, reaction conditions were performed as stated above with the exception of using 0.75 μg His–NEMO substrate and 1 μg His–xPIASy in a 40 μl reaction. End products were treated as above except SDS–PAGE gels were transferred and immunoblotted with goat anti-NEMO, rabbit anti-SUMO and His anti-mouse antibodies. For proteolysis of SUMO modified NEMO, SUMO reaction end products (40 μl reaction total) were incubated with 10 mM DTT at 30 °C for 15 minutes. 0.75 or 1.5 μg His-$SENP1^{CD}$ was then added to samples and incubated at 30 °C for 1 h. Reactions were terminated in SDS sample buffer and reaction products separated by SDS–PAGE gels.

To determine the effects of PIASy on NEMO sumoylation *in vitro*, pFlag–CMV-2 PIASy wild-type and pFlag–CMV-2 $PIASy^{C342/347A}$ expression constructs were transiently transfected into HEK293 cells. Cell extracts were prepared from these cells 24 h following transfection in immunoprecipitation buffer (20 mM Tris–HCl, 3 mM EDTA, 3 mM EGTA, 250 mM NaCl at pH 7.4). PIASy protein was immunoprecipitated by addition of anti-Flag antibody and Gamma Bind G-Sepharose. The immunoprecipitates were washed in high salt immunoprecipitation buffer (20 mM Tris–HCl, 3 mM EDTA, 3 mM EGTA and 500 mM NaCl at pH 7.4) with 10 mM sodium fluoride, 1 mM sodium orthovanadate, 2 mM DTT, 1 μg aprotinin per ml and 0.5 mM PMSF four times, followed by washing two times with *in vitro* sumoylation buffer (50 mM Tris and 5 mM $MgCl_2$ at pH 7.6) with 1 μg aprotinin per ml and 0.5 mM PMSF. Immune purified PIASy beads (20 μl) were added to the sumoylation reaction as stated above but incubated at 30 °C for 110 min.

To detect *in vivo* sumoylation of NEMO, cells were rinsed twice with PBS, harvested and pelleted by centrifugation. The cell pellets were then lysed in an immunoprecipiation buffer (20 mM Tris–HCl, 3 mM EDTA, 3 mM EGTA and 250 mM NaCl at pH 7.4) in the presence of 1% SDS, protease and phosphatase inhibitors[24], as well as 10 mM N-ethylmaleimide and 3 mM iodoacetamide. Samples were then boiled for 20 min to denature proteins and spun down to remove cellular debris and inputs from this lysate were taken. Samples were then diluted to 0.1% SDS with immunoprecipitation buffer. Myc–NEMO or endogenous NEMO was immunoprecipitated with anti-Myc or anti-NEMO antibody, respectively, on Protein G–Sepharose beads overnight and washed with immunoprecipitation buffer four times. Final immunoprecipitates were boiled in SDS sample buffer, separated by SDS–PAGE gels, transferred and immunoblotted as previously described[25].

Cell fractionation. Briefly, nuclear and cytoplasmic extracts were generated through hypotonic shock followed by nuclei extraction with salt as previously described[25].

Statistical analysis. Statistical analysis was performed with SigmaStat 3.0 software (SYSTAT Software, Inc., Richmond, CA). Mean values with equal variance were compared using and unpaired *t*-test. Mean values with unequal variance were compared using the Many-Whitney Rank Sum test.

Note: Supplementary Information is available on the Nature Cell Biology website.

ACKNOWLEDGMENTS

We thank Y. Azuma for generously providing recombinant purified *Xenopus* His–PIASy protein and *Xenopus* pET28a PIASy construct. We thank both M. Dasso and Y. Azuma for providing human PIASy antibody; K. Orth and S. Mukherjee for technical assistance and discussions regarding the development of *in vitro* sumoylation assays; E. Bresnick for the use of real time PCR equipment; P.-Y. Chang for assistance with quantitative RT–PCR analyses; S. Suryanarayanan and S. Shumway for generation of some NEMO deletion mutants. We also thank S. O'Connor for critical reading of the manuscript, C Berchtold for help with statistical analysis and the members of the Miyamoto lab for helpful discussions. This work is funded by the National Institutes of Health (NIH; T32GM008688) and Department of Defense BC044529 to A.M., Department of Defense BC010767 to S.W.-D., and NIH R01CA77474 and R01CA81065 and a Shaw Scientist Award from the Greater Milwaukee Foundation to S.M.

COMPETING FINANCIAL INTERESTS

The authors declare that they have no competing financial interests.

Published online at http://www.nature.com/naturecellbiology/
Reprints and permissions information is available online at http://npg.nature.com/reprintsandpermissions/

1. Gill, G. SUMO and ubiquitin in the nucleus: different functions, similar mechanisms? *Genes Dev.* **18,** 2046–2059 (2004).
2. Hay, R. T. SUMO: a history of modification. *Mol. Cell* **18,** 1–12 (2005).
3. Huang, T. T., Wuerzberger-Davis, S. M., Wu, Z. H. & Miyamoto, S. Sequential modification of NEMO/IKKγ by SUMO-1 and ubiquitin mediates NF-κB activation by genotoxic stress. *Cell* **115,** 565–576 (2003).
4. Wu, Z. H., Shi, Y., Tibbetts, R. S. & Miyamoto, S. Molecular linkage between the kinase ATM and NF-κB signaling in response to genotoxic stimuli. *Science* **311,** 1141–1146 (2006).
5. Pichler, A., Gast, A., Seeler, J.S., Dejean, A. & Melchior, F. The nucleoporin RanBP2 has SUMO1 E3 ligase activity. *Cell* **108,** 109–120 (2002).
6. Wuerzberger-Davis, S. M., Chang, P. Y., Berchtold, C. & Miyamoto, S. Enhanced G2–M arrest by NF-κB-dependent p21waf1/cip1 induction. *Mol. Cancer Res.* **3,** 345–353 (2005).
7. Bakkenist, C. J. & Kastan, M. B. DNA damage activates ATM through intermolecular autophosphorylation and dimer dissociation. *Nature* **421,** 499–506 (2003).
8. Hochstrasser, M. SP-RING for SUMO: new functions bloom for a ubiquitin-like protein. *Cell* **107,** 5–8 (2001).
9. Azuma, Y., Arnaoutov, A., Anan, T. & Dasso, M. PIASy mediates SUMO-2 conjugation of Topoisomerase-II on mitotic chromosomes. *EMBO J.* **24,** 2172–2182 (2005).
10. Sampson, D. A., Wang, M. & Matunis, M. J. The small ubiquitin-like modifier-1 (SUMO-1) consensus sequence mediates Ubc9 binding and is essential for SUMO-1 modification. *J. Biol. Chem.* **276,** 21664–21669 (2001).
11. Lin, D. *et al.* Identification of a substrate recognition site on Ubc9. *J. Biol. Chem.* **277,** 21740–21748 (2002).
12. Hayden, M. S. & Ghosh, S. Signaling to NF-κB. *Genes Dev.* **18,** 2195–2224 (2004).
13. Riley, P.A. Free radicals in biology: oxidative stress and the effects of ionizing radiation. *Int. J. Radiat. Biol.* **65,** 27–33 (1994).
14. Pham, N.A. & Hedley, D.W. Respiratory chain-generated oxidative stress following treatment of leukemic blasts with DNA-damaging agents. *Exp. Cell Res.* **264,** 345–352 (2001).
15. Mikkelsen, R.B. & Wardman, P. Biological chemistry of reactive oxygen and nitrogen and radiation-induced signal transduction mechanisms. *Oncogene* **22,** 5734–5754 (2003).
16. England, K., O'Driscoll, C. & Cotter, T.G. Carbonylation of glycolytic proteins is a key response to drug-induced oxidative stress and apoptosis.*Cell Death Differ.* **11,** 252–260 (2004).
17. Brummelkamp, T. R., Nijman, S. M., Dirac, A. M. & Bernards, R. Loss of the cylindromatosis tumour suppressor inhibits apoptosis by activating NF-κB. *Nature* **424,** 797–801 (2003).
18. Liu, B. *et al.* Negative regulation of NF-κB signaling by PIAS1. *Mol. Cell Biol.* **25,** 1113–1123 (2005).
19. Jang, H. D., Yoon, K., Shin, Y. J., Kim, J. & Lee, S. Y. PIAS3 suppresses NF-κB-mediated transcription by interacting with the p65/RelA subunit. *J. Biol. Chem.* **279,** 24873–24880 (2004).
20. Janssens, S., Tinel, A., Lippens, S. & Tschopp, J. PIDD mediates NF-κB activation in response to DNA damage. *Cell* **123,** 1079–1092 (2005).
21. Karin, M. & Greten, F. R. NF-κB: linking inflammation and immunity to cancer development and progression. *Nature Rev. Immunol.* **5,** 749–759 (2005).
22. Aggarwal, B. B. Nuclear factor-κB: the enemy within. *Cancer Cell* **6,** 203–208 (2004).
23. Huang, T. T. *et al.* NF-κB activation by camptothecin. A linkage between nuclear DNA damage and cytoplasmic signaling events. *J. Biol. Chem.* **275,** 9501–9509 (2000).
24. Huang, T. T., Feinberg, S. L., Suryanarayanan, S. & Miyamoto, S. The zinc finger domain of NEMO is selectively required for NF-κB activation by UV radiation and topoisomerase inhibitors. *Mol. Cell Biol.* **22,** 5813–5825 (2002).
25. Miyamoto, S., Seufzer, B. J. & Shumway, S. D. Novel IκBα proteolytic pathway in WEHI231 immature B cells. *Mol. Cell Biol.* **18,** 19–29 (1998).
26. O'Connor, S., Shumway, S. D., Amanna, I. J., Hayes, C. E. & Miyamoto, S. Regulation of constitutive p50/c-Rel activity via proteasome inhibitor-resistant IκBα degradation in B cells. *Mol. Cell Biol.* **24,** 4895–4908 (2004).

nature cell biology

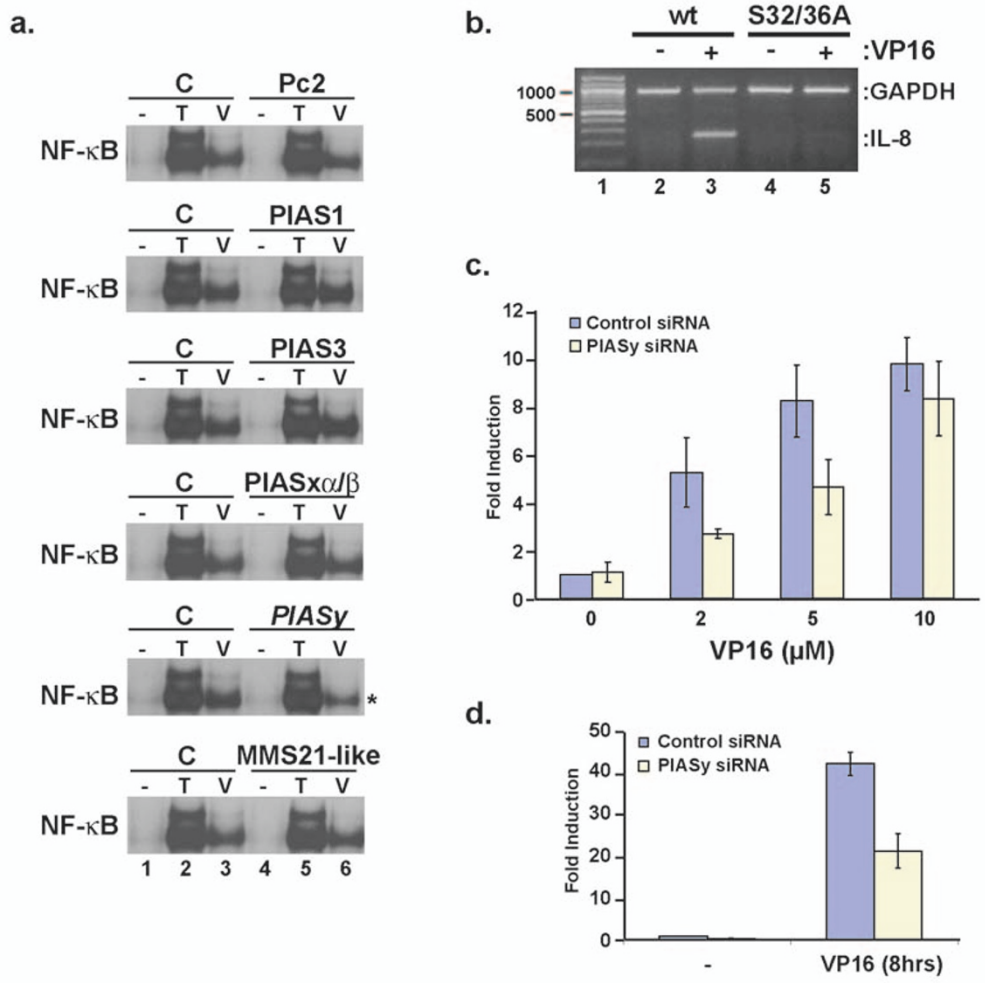

Figure S1: **a.** HEK293 cells were transfected with control or siRNAs against different SUMO ligases. Cells were treated with 10 μM VP16 for 60 minutes or 10ng/mL TNFα for 15 minutes. Total cell extracts were made and NF-κB activity was measured using EMSA. **b.** HEK293 and HEK293 IκBα-S32/36A stable cells were treated with 10 μM VP16 for 3 hours. RNA from cells was isolated and RT-PCR was performed using IL-8 and GAPDH primers. **c.** HEK293 cells were transfected with control or PIASy siRNAs and treated with increasing doses of VP16 for 3 hours. RNA was isolated and analyzed for IκBα using quantitative real time RT-PCR. **d.** CEM cells were transfected with control or PIASy siRNAs and treated with 10 μM VP16 for 6 hours. Samples were analyzed for p21 using quantitative real time RT-PCR.

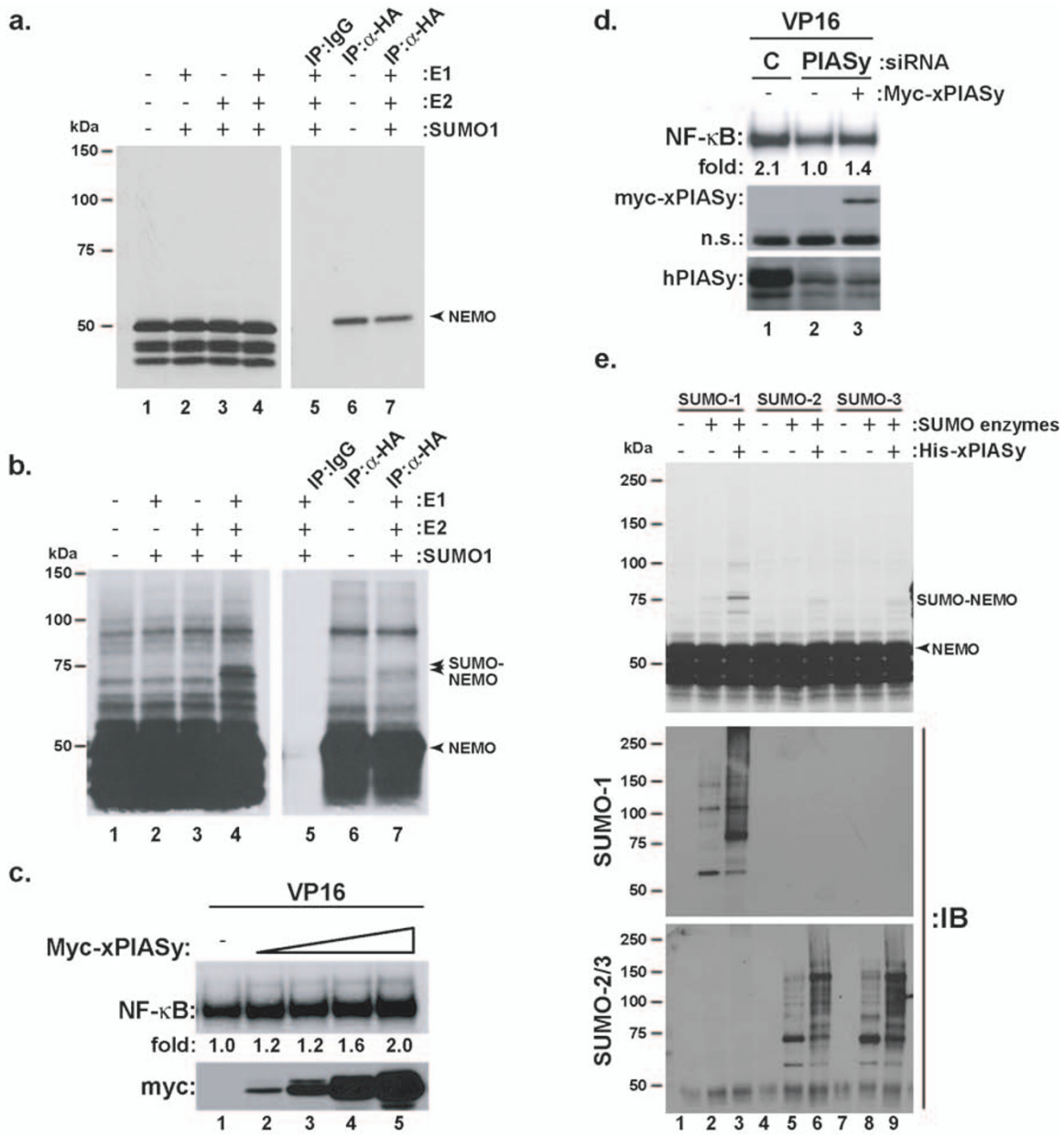

Figure S2: **a.** Light exposure of *in vitro* translated NEMO assay peformed in b. **b.** *In vitro* translated ^{35}S-methionine-labeled HA-NEMO was added to *in vitro* SUMOylation reaction. SUMO E1 and E2 were added as stated in materials and methods. Samples were run on an SDS-PAGE gel, fixed, and exposed to film. Alternatively, reaction products were boiled in 1%SDS and immunoprecipitated with an anti-HA antibody and analyzed as stated above. **c.** HEK293 cells were transfected with 0.15, 0.5, 1.5, and 4.0 µg of *Xenopus* PIASy (Myc-xPIASy) DNA. Cells were treated with 10 µM VP16 for 75 minutes. Total cells extracts were measured for NF-κB activity by EMSA. **d.** HEK293 cells were transfected with PIASy siRNA (oligo#2) and 0.2 µg Myc-xPIASy DNA. Cells were treated with 10 µM VP16 for 120 minutes. NF-κB activity was measured as in c. **e.** *In vitro* translated ^{35}S-methionine-labeled HA-NEMO was added to SUMO reaction as in a. Reactions were performed in the presence of different SUMO protein isoforms: SUMO-1 (lanes 1-3), SUMO-2 (lanes 4-6), or SUMO-3 (lanes 7-9). 0.5 µg of His-xPIASy was added to the SUMO reaction. The mixture was incubated at 30 °C for 75 minutes and terminated in 2xSDS sample buffer. Samples were run on an SDS-PAGE gel, fixed, and exposed to film. Alternatively, terminated reaction end products were western blotted and probed with mouse anti-SUMO-1 and rabbit anti-SUMO-2 (which also recognizes SUMO-3), showing that His-xPIASy can promote modification of reticulocyte proteins by SUMO-1, -2 and –3 even though it preferentially promotes SUMO-1 modification of NEMO.

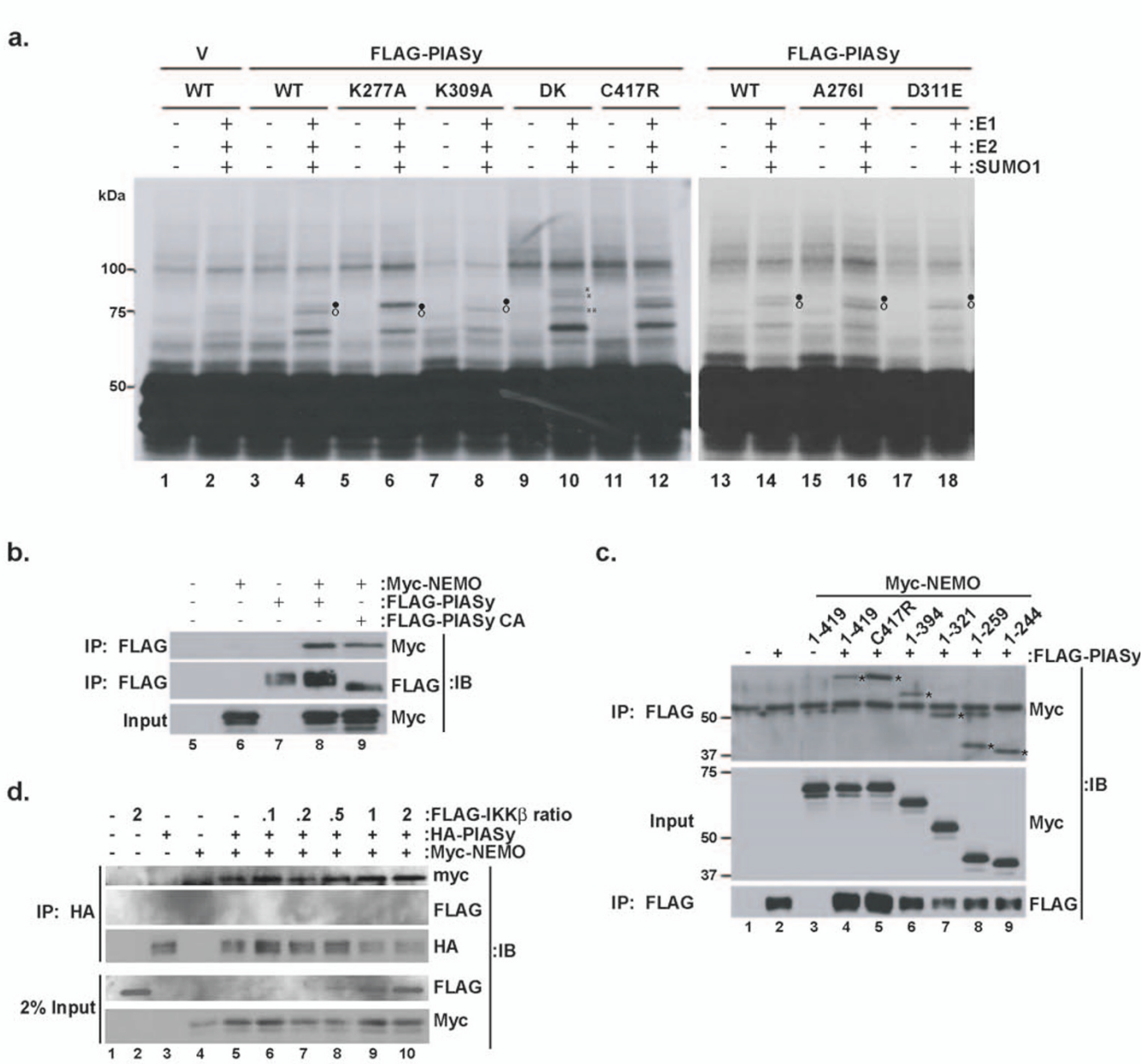

Figure S3: **a.** A similar experiment as shown in Figure 3g was performed using immunopurified human Flag-PIASy instead of His-xPIASy. The SUMOylation banding patters of different NEMO mutants are nearly indistinguishable from those shown in Figure 3g. **b.** HEK293 cells were transfected with Flag-PIASy, Myc-NEMO, and Flag-PIASy-CA. Cells were harvested and lysed, and cell extracts were immunoprecipitated using anti-Flag antibody. Western blotting was performed using anti-Myc and anti-FLAG antibodies. **c.** HEK293 cells were transfected with Flag-PIASy and Myc-NEMO mutants. Cells were immunoprecipitated with an anti-Flag antibody and probed with an HRP-conjugated anti-Myc antibody. **d.** HEK293 cells were transiently transfected with HA-PIASy, Flag-IKKβ, and Myc-NEMO constructs. Flag-IKKβ was titrated in increasing DNA ratios with PIASy. Cell extracts were immunoprecipitated with an anti-HA antibody and probed with anti-Flag and HRP-conjugated anti-HA and anti-Myc antibodies.

Mabb et al-Supplemental Figure S4

RT-PCR Primers	+ strand	- strand
GAPDH:	5'-GTCTTACTCCTTGGAGGCCATG-3'	5'-ACCCCTTCATTGACCTCAACTAC-3'
Pc2:	5'-GAGAACATCCTGGACCCCAGGC-3'	5'-CTGGGCGCCTCCTTGTGGCCGC-3'
PIAS1:	5'-GAACTCCAAGTACTGTTGGGCT-3'	5'-CGGATGGACTGGGTGAAGAGCT-3'
PIAS3:	5'-GGTGCTTCTTGGCTTTGCTGGC-3'	5'-GCTGGCTAGAAGTGGATGCAAG-3'
PIASxα:	5'-CCAGCCAACCGTGTACAAAAATAG-3'	5'-TTCTTTGTTCTCCTGGCAAATC-3'
PIASxβ:	5'-CCAGCCAACCGTGTACAAAAATAG-3'	5'-CTGGTGGTGGTGACAGACGTAC-3'
PIASy:	5'-CTTTAATATGCTGGATGAGCTG-3'	5'-CTCCTTGACCAGTGCCTTGCAC-3'
AL136/MMS21-like:	5'-TGCAGGTCAGCGTCAATGCCAC-3'	5'-GCACTTCAGGGACACCTTGATA-3'
IL-8:	5'-TGCAGCTCTGTGTGAAGG-3'	5'-CTCAGCCCTCTTCAAAAAC-3'
siRNA Oligonucleotides		
Control:	5'-UACCGUCUCCACUUGAUCGdTdT-3'	5'-CGAUCAAGUGGAGACGGUAdTdT-3'
PIASy oligo #2:	5'-CAAGACAGGUGGAGUUGAUUU-3'	5'-PAUCAACUCCACCUGUCUUGUU-3'
PIASy oligo #4:	5'-AAGCUGCCGUUCUUUAAUAUU-3'	5'-PUAUUAAAGAACGGCAGCUUUU-3'
Real Time RT-PCR Primers		
GAPDH:	5'-GAAGGTCGG-AGTCAACGGATTT-3'	5'-GAATTTGCCATGGGTGGAAT-3'
IL-8:	5'-GCAGCTCTGTGTGAAGGTGC-3'	5'-CGCAGTGTGGTCCACTCTCA-3'
IκBα:	5'-GCTACCAACTACAATGGCCACA-3'	5'-TAGCCATGGATAGAGGCTAAGTGTAGA-3'
p21:	5'-GCAGACCAGCATGACAGATTTC-3'	5'-GCGGATTAGGGCTTCCTCTT-3'

Figure S4: Sequences of RT-PCR primers and some of the siRNA oligos used in this study.

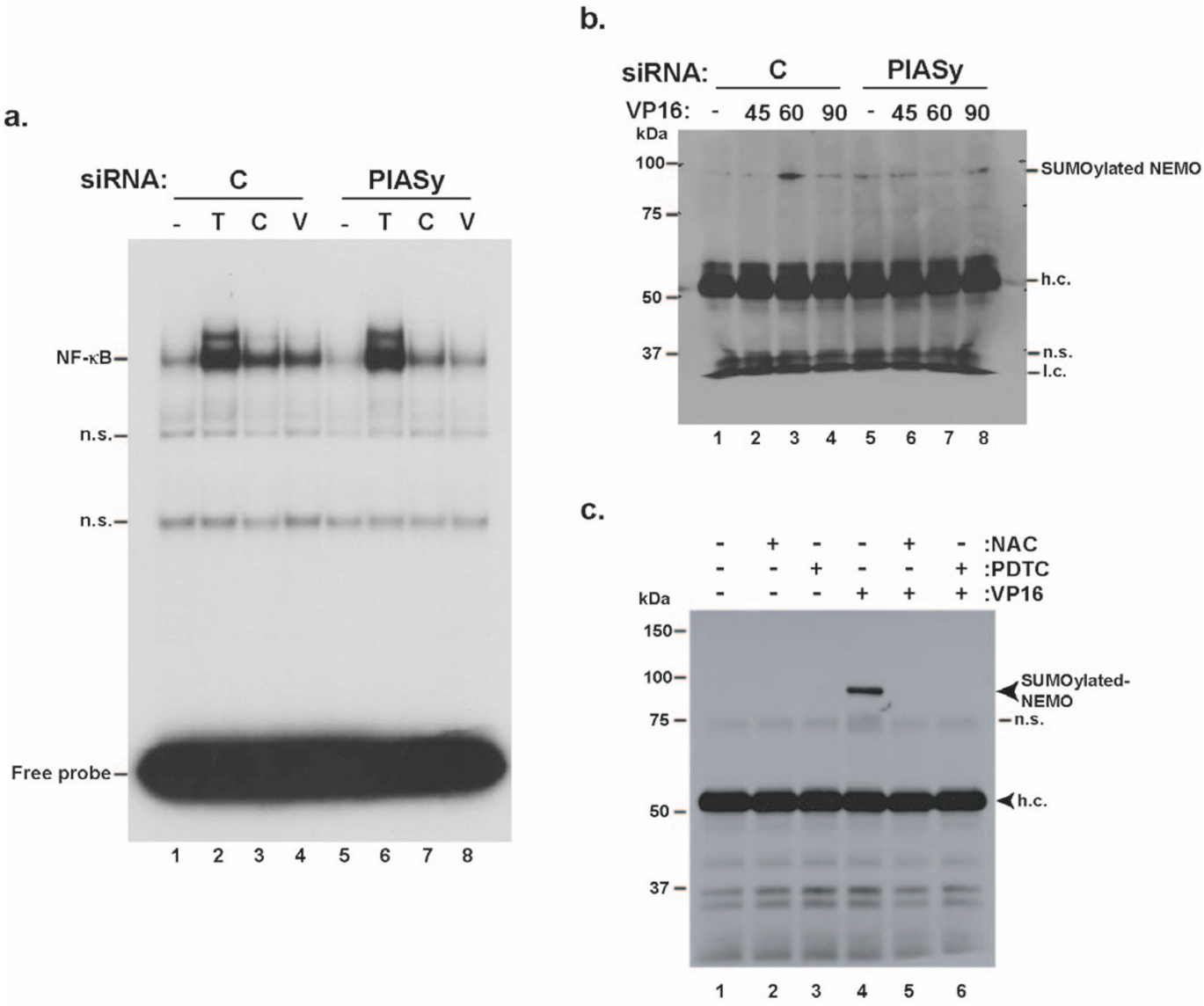

Figure S5: Full scans of original EMSA gel and Western blots. **a.** Full scan of the top panel of Figure 1b EMSA gel. n.s. refers to a nonspecific band, **b.** Full scan of the top panel of Figure 2a SUMO-1 Western blot. h.c. refers to IgG heavy chain and l.c. refers to light chain. **c.** Full scan of the top panel of Figure 5a SUMO-1 Western blot.